

Compact X-ray Free-Electron Laser from a Laser-Plasma Accelerator Using a Transverse-Gradient Undulator

Zhirong Huang,¹ Yuantao Ding,¹ and Carl B. Schroeder²

¹SLAC National Accelerator Laboratory, Menlo Park, California 94025, USA

²Lawrence Berkeley National Laboratory, Berkeley, California 94720, USA

(Received 13 July 2012; published 12 November 2012)

Compact laser-plasma accelerators can produce high energy electron beams with low emittance, high peak current but a rather large energy spread. The large energy spread hinders the potential applications for coherent free-electron laser (FEL) radiation generation. We discuss a method to compensate the effects of beam energy spread by introducing a transverse field variation into the FEL undulator. Such a transverse gradient undulator together with a properly dispersed beam can greatly reduce the effects of electron energy spread and jitter on FEL performance. We present theoretical analysis and numerical simulations for self-amplified spontaneous emission and seeded extreme ultraviolet and soft x-ray FELs based on laser plasma accelerators.

DOI: 10.1103/PhysRevLett.109.204801

PACS numbers: 41.60.Cr, 41.75.Jv, 52.38.Kd

The advent of x-ray free-electron lasers (FELs) represents a revolution in light source development that enables the simultaneous probe of both the ultrasmall and the ultrafast worlds [1]. The first soft x-ray FEL facility, FLASH at DESY, has been in operation for users since 2005 [2]. The first hard x-ray FEL facility, the Linac Coherent Light Source at SLAC [3], became operational in 2009. More recently, the SACLA at SPring-8 [4] started its user program beginning in 2012. These are remarkable scientific facilities in size (hundreds to thousands of meters long) and in user capacities (hundreds of users annually). A few more such facilities will come online in this decade [5]. Nevertheless, it is very desirable to develop compact x-ray FELs that are similar in characteristics but are much smaller in footprint.

Laser plasma accelerators (LPAs) have made tremendous progress in generating high-energy (~ 1 GeV), high peak current (~ 10 kA), and low-emittance (~ 0.1 μm) beams [6,7]. Such an accelerator was used to produce soft x-ray spontaneous undulator radiation [8], and active research and development efforts have been pursued to develop compact FELs [9,10] based on these novel accelerators. Nevertheless, due to the challenges in controlling the injection process, LPA beams have rather large energy spread, typically on a few percent level. Such energy spread hinders the short-wavelength FEL application.

The goal of this Letter is to point out that a transverse gradient undulator together with a properly dispersed beam is capable of overcoming the large energy spread of LPAs for short-wavelength FEL amplification. Using one-dimensional (1D) analysis and three-dimensional (3D) simulations, we show how LPAs can be used to drive extreme ultraviolet (EUV) and soft x-ray FELs in short undulators. The resulting radiation pulses can be multi-gigawatt in power, a few femtosecond in duration, and have good transverse and temporal coherence properties.

The effect of beam energy spread on FELs can be best understood by the undulator resonant wavelength

$$\lambda_r = \frac{\lambda_u}{2\gamma^2} \left(1 + \frac{K_0^2}{2} \right). \quad (1)$$

Here, λ_u and K_0 are the undulator period and the strength parameter, respectively. If there is a spread in the average beam energies $\gamma_0 mc^2$, it will lead to a spread of the resonant condition and degrade the FEL gain. For a high-gain FEL, the typical requirement is

$$\sigma_\delta = \frac{\sigma_\gamma}{\gamma_0} \ll \rho = \left[\frac{1}{16} \frac{I_0}{I_A} \frac{K_0^2 [\text{JJ}]^2}{\gamma_0^3 \sigma_x^2 k_u^2} \right]^{1/3}, \quad (2)$$

where ρ is the FEL Pierce parameter [11], $[\text{JJ}] = [J_0(\xi) - J_1(\xi)]$ with $\xi = K_0^2/(4 + 2K_0^2)$ for a planar undulator, $I_A \approx 17$ kA is the Alfvén current, $k_u = 2\pi/\lambda_u$, I_0 is the beam peak current, and σ_x is the average rms transverse beam size in the undulator.

Smith and co-workers at Stanford proposed a “transverse gradient wiggler (undulator)” (TGU) to reduce the sensitivity to electron energy variations for FEL oscillators [12]. The idea is illustrated in Fig. 1. By canting the magnetic poles, one can generate a linear x dependence of the vertical undulator field so that

$$\frac{\Delta K}{K_0} = \alpha x. \quad (3)$$

Consider dispersing the electron beam horizontally according to its energy such that $x = \eta \Delta\gamma/\gamma_0$. By choosing the dispersion function

$$\eta = \frac{2 + K_0^2}{\alpha K_0^2} \quad (4)$$

and keeping it constant in the TGU, the change in electron’s energy is now exactly compensated by the change in

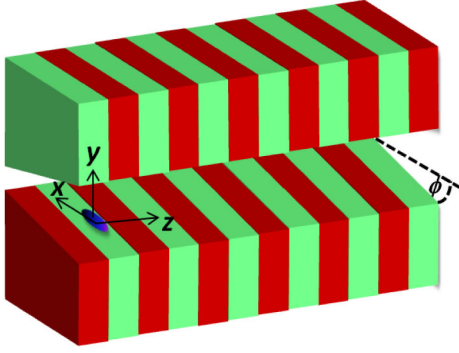


FIG. 1 (color online). Transverse gradient undulator by canting the magnetic poles. Each pole is canted by an angle ϕ with respect to the xz plane. The higher energy electrons are dispersed to the higher field region (positive x) to match the FEL resonant condition.

the magnetic field so that every electron satisfies the resonant condition Eq. (1) in the undulator. For a full cant angle $2\phi \approx \Delta y/(\Delta x)$, the gradient parameter is

$$\alpha = 2\phi \frac{1}{K_0} \frac{\partial K_0}{\partial y} = 2\phi \left(\frac{5.47}{\lambda_u} - 3.6 \frac{g}{\lambda_u^2} \right), \quad (5)$$

where the last step uses Halbach's formula [13] for hybrid undulators and g is the average gap of the canted poles. We note that the TGU concept has been recently discussed to improve the spontaneous undulator radiation spectrum by using a superconducting (SC) undulator [14]. The advantage of a superconducting undulator is the combination of smaller period, larger magnetic field and higher transverse gradient.

The TGU analysis of Refs. [12,15] was aimed at low-gain FELs. Here we study high-gain FELs which are more relevant for LPAs. We first use the 1D FEL model and ignore 3D effects. In a normal undulator, the gain length dependence on the (Gaussian) energy spread can be described by

$$L_G \approx \frac{\lambda_u}{4\pi\sqrt{3}\rho} \left(1 + \frac{\sigma_\delta^2}{\rho^2} \right). \quad (6)$$

This formula yields the right asymptotic behaviors for both $\sigma_\delta \ll \rho$ and $\sigma_\delta \gg \rho$ [16] and agrees with the numerical solution of the 1D FEL dispersion relation.

For a transverse gradient undulator, the beam is dispersed in the horizontal direction with an increased beam size. This reduces the beam density and the coupling to the radiation through the FEL parameter ρ . We can define an effective ρ for TGU as

$$\rho_T = \rho \left(1 + \frac{\eta^2 \sigma_\delta^2}{\sigma_x^2} \right)^{-1/6}. \quad (7)$$

Because of the transverse field gradient, an intrinsic horizontal beam size will also induce an effective energy spread in a TGU as

$$\sigma_\delta^{\text{eff}} = \frac{K_0^2}{2 + K_0^2} \frac{\sigma_K}{K_0} = \frac{K_0^2}{2 + K_0^2} \alpha \sigma_x. \quad (8)$$

The intrinsic beam size is determined by the horizontal emittance ε_x and the beta function β . For a relatively short undulator of length L_u considered here for LPAs without external focusing, it is reasonable to take $\beta \approx L_u/2$, and hence $\sigma_x = \sqrt{\varepsilon_x L_u/2}$ in Eq. (8). The 1D gain length for a TGU equivalent to Eq. (6) is then

$$L_G^T \approx \frac{\lambda_u}{4\pi\sqrt{3}\rho_T} \left[1 + \left(\frac{K_0^2}{2 + K_0^2} \right)^2 \frac{\alpha^2 \varepsilon_x L_u}{2\rho_T^2} \right]. \quad (9)$$

Let us consider a LPA operating between 500 MeV to 1 GeV with the normalized emittance $\gamma_0 \varepsilon_x \sim 0.1 \mu\text{m}$ and a peak current of $I_0 \sim 5$ to 10 kA. For a few-meter undulator length, we can expect $\sigma_x \sim 15 \mu\text{m}$. Let us take $\lambda_u = 1$ to 2 cm, $K \sim 2$ in order to reach EUV and soft x-ray wavelengths. This leads to the estimation $\rho \sim 5 \times 10^{-3}$. We also assume the transverse gradient parameter $\alpha \sim 100 \text{ m}^{-1}$ (see Table I below for more details), then the dispersion is $\eta \approx 1.5 \text{ cm}$. If we define the gain length ratios as the gain lengths predicted from Eqs. (6) and (9) over the ideal gain length $\lambda_u/(4\pi\sqrt{3}\rho)$, Fig. 2 shows these ratios vs rms energy spread generated by the LPA in units of ρ . We conclude that TGU can significantly reduce the gain length when $\sigma_\delta > \rho$ for these parameters.

Another method to reduce the gain length of a large energy spread beam is by decompressing the electron bunch longitudinally [17]. Decompression reduces the energy spread over an FEL slice at the expense of decreasing the peak current. Figure 2 shows the estimated gain length using this approach with a decompression factor of 10. Although a similar gain length reduction may be obtained this way, the transverse gradient undulator offers four distinct advantages over the decompression method: (i) Shorter x-ray pulse length (a few fs in duration) and higher peak x-ray power; (ii) smaller radiation bandwidth;

TABLE I. Electron beam and undulator parameters used to study transverse gradient undulator for compact EUV and soft x-ray FELs.

Parameter	Symbol	EUV	X-ray
Beam energy	$\gamma_0 mc^2$	500 MeV	1 GeV
Norm. transv. emittance	$\gamma_0 \varepsilon_x$	0.1 μm	0.1 μm
Peak current	I_0	5 kA	10 kA
Flattop bunch duration	T	10 fs	5 fs
Rel. rms energy spread	σ_δ	2%	1%
Undulator type		Hybrid	SC
Undulator period	λ_u	2.18 cm	1 cm
Undulator length	L_u	5 m	5 m
Undulator parameter	K_0	1.85	2
Transverse gradient	α	43 m^{-1}	150 m^{-1}
Horizontal dispersion	η	3.7 cm	1 cm
Resonant wavelength	λ_r	31 nm	3.9 nm

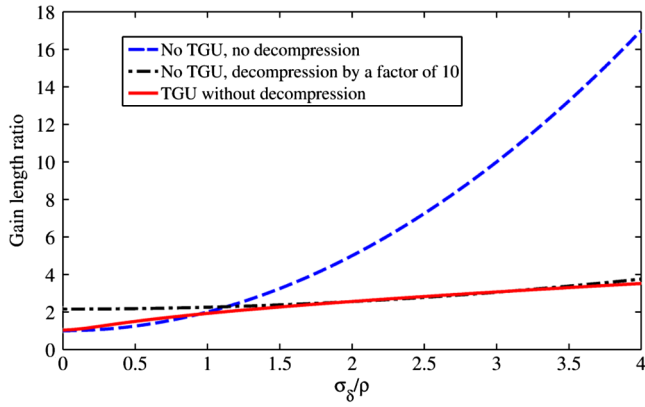


FIG. 2 (color online). Gain length ratio vs rms energy spread for a normal undulator without decomposition (dashed blue), with a factor of 10 decomposition (dashed-dotted black), and for a transverse gradient undulator without decomposition (solid red).

(iii) enable direct or self-seeding by reducing the effect of large energy spread; (iv) stable central wavelength in the presence of shot-to-shot energy jitters.

A TGU will have a net bending field since a wiggling electron sees a stronger B_u in the first half of the undulator period than the second half. It can be corrected by a uniform dipole field B_c or a series of correctors. The field strength of B_c is estimated to be on the order of 1 Gauss for a high-energy (~ 1 GeV) electron beam.

3D effects such as diffraction and transverse modes can be studied by GENESIS simulations [18]. For this purpose, GENESIS is modified to include a linear gradient term for the undulator field but the net deflection is ignored (or corrected). TGU also introduces a weak horizontal focusing with the betatron wavelength $4\pi\gamma_0\sqrt{1 + K_0^2/2}/(\alpha K_0^2)$ [15]. For the numerical examples shown below, the horizontal betatron wavelength is on the order of 70 m to 200 m and is much longer than the 5-m undulator under consideration. Thus, this effect is also neglected in our simulations.

We first consider an EUV FEL example that is very close to the ongoing LBNL laser plasma experiment [9]. A 5-m THUNDER undulator [19] is available after the plasma accelerator for FEL studies. To produce the required transverse gradient, we assume that each magnetic pole can be canted from the flat geometry by $\phi = 0.1$ rad [20]. For the average magnetic gap $g = 4.8$ mm and period $\lambda_u = 2.18$ cm, the corresponding transverse gradient is $\alpha = 43$ m $^{-1}$ according to Eq. (5). This gradient may not be the optimal but is sufficient to demonstrate the TGU advantage. Table I lists the beam and undulator parameters for such an EUV FEL.

Figure 3 shows the simulated FEL power around 31 nm along the THUNDER undulator for the case of flat poles (black) and the canted poles with $2\phi = 0.2$ rad (red). For a self-amplified spontaneous emission (SASE) FEL, the

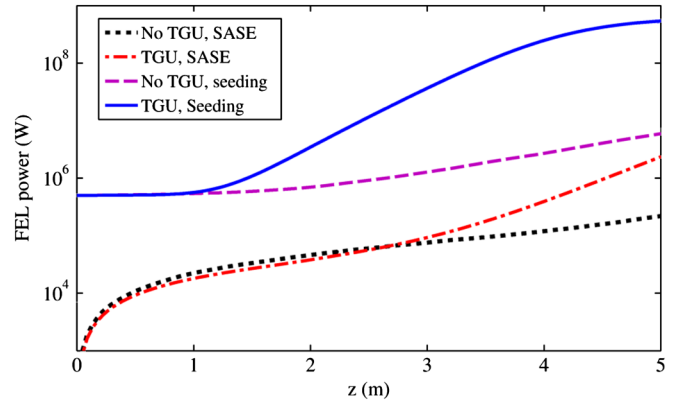


FIG. 3 (color online). SASE FEL power around 31 nm for a normal THUNDER undulator (dotted black) and for a TGU (dashed-dotted red). Seeded FEL power for a normal THUNDER undulator (dashed magenta) and for a TGU (solid blue).

power improvement of the TGU THUNDER is about one order of magnitude for a 5-m device even though this length is much shorter than the FEL saturation length. At this EUV radiation wavelength, seeding with a coherent source from high-harmonic generation in gas is feasible. We then assume 500 kW seed power with the rms spot size of about $50 \mu\text{m}$ at the entrance of the undulator. Figure 3 shows that seeding works much more effectively with TGU (blue) than without TGU (magenta) because of the much reduced energy spread effects, and that the seeded FEL reaches saturation within 5-m THUNDER undulator. Figure 4 shows typical single-shot spectra of these four cases.

Due to the large horizontal beam size ($740 \mu\text{m}$ in this example), the SASE FEL develops multiple transverse modes for the THUNDER TGU considered here [see Fig. 5(a)]. The transverse coherence can be drastically

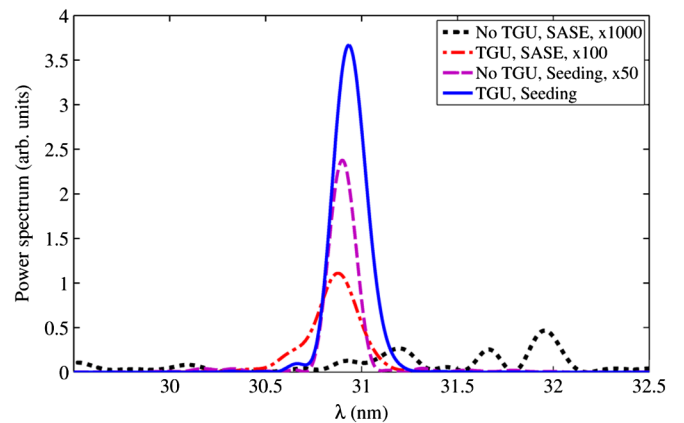


FIG. 4 (color online). Typical single-shot spectra of SASE FEL for a normal THUNDER undulator (dotted black) and for a TGU (dashed-dotted red). Seeded FEL spectra for a normal THUNDER undulator (dashed magenta) and for a TGU (solid blue).

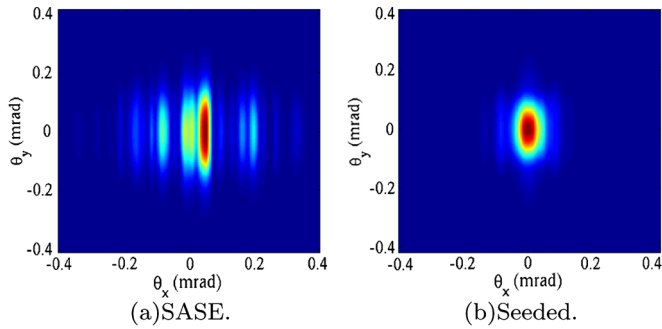


FIG. 5 (color online). Transverse mode pattern for a SASE and a seeded FEL at 31 nm based on the THUNDER TGU.

improved by seeding, as shown in Fig. 5(b). As we will show in the next example, the transverse mode pattern of SASE can be improved if the transverse gradient of the undulator is increased, even in the absence of seeding.

We now consider a compact soft x-ray FEL example using 1 GeV laser plasma beams that have been demonstrated at LBNL [21] and elsewhere [22,23]. To reach the important “water window” wavelengths, we consider using the SC undulator described in Ref. [14] (see Table I) that also reaches very large transverse gradient $\alpha \approx 300 \text{ m}^{-1}$. The detailed parameter list for this set of simulations can be found in Table I. Figure 6 shows the FEL power around 3.9 nm for the case of a normal SC undulator (blue) as well as a SC undulator with $\alpha = 150 \text{ m}^{-1}$ (red). We see that the TGU improves the SASE power by about two orders of magnitude and reaches power saturation within 5-m undulator distance. For comparison, we also show in Fig. 6 a case of decompressed beam with a peak current of 1.5 kA and a slice energy spread of 0.15% (black). Although the gain length of the decompressed beam is similar to that of the TGU, it saturates at lower power level due to the lower peak current. Figure 7 shows the comparison of typical single shot spectra for the three

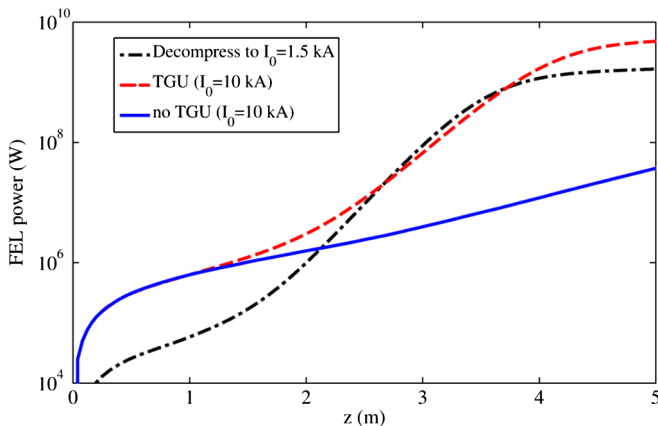


FIG. 6 (color online). FEL power around 3.9 nm for a normal undulator without decompression (solid blue), with a factor of 7 decompression (dashed dotted black), and for a transverse gradient undulator without decompression (dashed red).

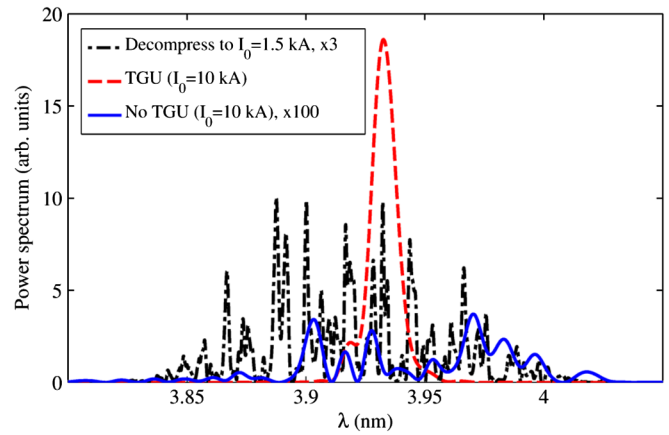


FIG. 7 (color online). Typical single-shot spectra of SASE for a normal undulator without decompression (solid blue), with a factor of 7 decompression (dashed dotted black), and for a transverse gradient undulator without decompression (dashed red).

cases. Because of the very short electron pulse duration ($\sim 5 \text{ fs}$) without decompression, the TGU SASE forms a single coherent spike while the decompressed beam generates multiple spikes with its rms bandwidth close to 2%. Figures 8(a) and 8(b) show the SASE transverse mode pattern in the absence of decompression. Without TGU, the transverse coherence is very poor because of the large energy spread and relatively low gain. With TGU, good transverse coherence ($\sim 50\%$) is established because the stronger transverse gradient allows for a weakly dispersed beam ($100 \mu\text{m}$ horizontal rms beam size).

One additional advantage of TGU is that the FEL wavelength is insensitive to the electron energy jitter. At present, LPAs generate beams with a few percent energy jitter. Without TGU, this large energy jitter directly maps into SASE wavelength jitter. TGU can potentially reduce or eliminate this energy jitter completely.

In summary, we have demonstrated the significant advantage of using TGUs to enhance the short-wavelength FEL performance of laser-plasma accelerators with 1D analysis and 3D simulations. There are several practical effects that were not included in these simple considerations. They

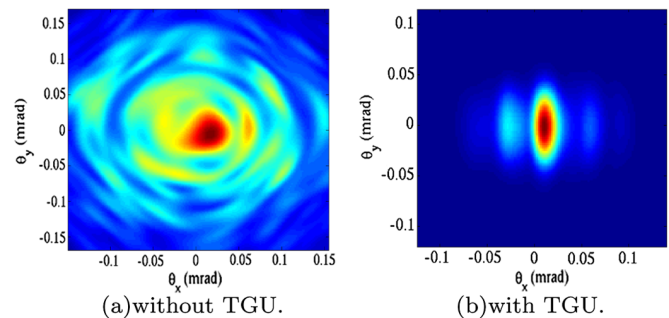


FIG. 8 (color online). Transverse mode pattern for a SASE FEL at 3.9 nm.

include electron energy correlation with bunch longitudinal coordinate and the method of generating the required beam dispersion. These and other effects should be taken into account in the design and optimization of the TGU experiments. We believe the study presented here and further investigations will make TGU a viable option to drive short-wavelength FELs for beams with relatively large energy spreads or jitters from laser-plasma and other types of accelerators.

We would like to thank E. Esarey, W. Fawley, M. Fuchs, J. Galayda, W. Leemans, A. Marinelli, H.-D. Nuhn, S. Reiche, and K. Robinson for useful discussions. This work was supported by Department of Energy Contract No. DE-AC02-76SF00515 and No. DE-AC02-05CH11231.

-
- [1] K. Gaffney and H. Chapman, *Science* **316**, 1444 (2007).
 - [2] W. Ackermann *et al.*, *Nature Photon.* **1**, 336 (2007).
 - [3] P. Emma *et al.*, *Nature Photon.* **4**, 641 (2010).
 - [4] T. Ishikawa *et al.*, *Nature Photon.* **6**, 540 (2012).
 - [5] B. McNeil and N. Thompson, *Nature Photon.* **4**, 814 (2010).
 - [6] E. Esarey, C. Schroeder, and W. Leemans, *Rev. Mod. Phys.* **81**, 1229 (2009).
 - [7] V. Malka, *Phys. Plasmas* **19**, 055501 (2012).
 - [8] M. Fuchs *et al.*, *Nat. Phys.* **5**, 826 (2009).
 - [9] C. Schroeder *et al.*, *Proceedings of FEL 2006* (Berlin, Germany, 2006) p. 455
 - [10] F. Gruner *et al.*, *Appl. Phys. B* **86**, 431 (2007).
 - [11] R. Bonifacio, C. Pellegrini, and L.M. Narducci, *Opt. Commun.* **50**, 373 (1984).
 - [12] T. Smith, J.M.J. Madey, L.R. Elias, and D.A.G. Deacon, *J. Appl. Phys.* **50**, 4580 (1979).
 - [13] K. Halbach, *J. Phys. (Paris)* **44**, C1-211 (1983).
 - [14] G. Fuchert, A. Bernhard, S. Ehlers, P. Peiffer, R. Rossmanith, and T. Baumbach, *Nucl. Instrum. Methods Phys. Res., Sect. A* **672**, 33 (2012).
 - [15] N. Kroll, P. Morton, M. Rosenbluth, J. Eckstein, and J. Madey, *IEEE J. Quantum Electron.* **17**, 1496 (1981).
 - [16] E.L. Saldin, E.A. Schneidmiller, and M.V. Yurkov, *The Physics of Free Electron Lasers* (Springer, Berlin, 2000).
 - [17] A.R. Maier, A. Meseck, S. Reiche, C.B. Schroeder, T. Seggebrock, and F. Grüner, *Phys. Rev. X*, **2**, 031019 (2012).
 - [18] S. Reiche, *Nucl. Instrum. Methods Phys. Res., Sect. A* **429**, 243 (1999).
 - [19] K. Robinson, D. Quimby, and J. Slater, *IEEE J. Quantum Electron.* **23**, 1497 (1987).
 - [20] K. Robinson (private communications).
 - [21] W. Leemans, B. Nagler, A.J. Gonsalves, C. Tóth, K. Nakamura, C.G.R. Geddes, E. Esarey, C.B. Schroeder, and S.M. Hooker, *Nat. Phys.* **2**, 696 (2006).
 - [22] S. Kneip *et al.*, *Phys. Rev. Lett.* **103**, 035002 (2009).
 - [23] J.S. Liu *et al.*, *Phys. Rev. Lett.* **107**, 035001 (2011).